Virtual Target-Based Overtaking Decision, Motion Planning, and Control of Autonomous Vehicles

HEUNGSEOK CHAE AND **KYONGSU YI**

Department of Mechanical and Aerospace Engineering, Seoul National University, Seoul 08826, South Korea

Corresponding author: Kyongsu Yi (kyi@snu.ac.kr)

ABSTRACT This paper describes the design, implementation, and evaluation of a virtual target-based overtaking decision, motion planning, and control algorithm for autonomous vehicles. Both driver acceptance and safety, when surrounded by other vehicles, must be considered during autonomous overtaking. These are considered through safe distance based on human driving behavior. Since all vehicles cannot be equipped with a vehicle to vehicle communications at present, autonomous vehicles should perceive the surrounding environment based on local sensors. In this paper, virtual targets are devised to cope with the limitation of cognitive range. A probabilistic prediction is adopted to enhance safety, given the potential behavior of surrounding vehicles. Then, decision-making and motion planning has been designed based on the probabilistic prediction-based safe distance, which could achieve safety performance without a heavy computational burden. The algorithm has considered the decision rules that drivers use when overtaking. For this purpose, concepts of target space, demand, and possibility for lane change are devised. In this paper, three driving modes are developed for active overtaking. The desired driving mode is decided for safe and efficient overtaking. To obtain desired states and constraints, intuitive motion planning is conducted. A stochastic model predictive control has been adopted to determine vehicle control inputs. The proposed autonomous overtaking algorithm has been evaluated through simulation, which reveals the effectiveness of virtual targets. Also, the proposed algorithm has been successfully implemented on an autonomous vehicle and evaluated via real-world driving tests. Safe and comfortable overtaking driving has been demonstrated using a test vehicle.

INDEX TERMS Autonomous vehicles, autonomous driving, decision-making, motion planning, vehicle control, overtaking, lane change, virtual target.

I. INTRODUCTION

The final goal of autonomous vehicle (AV) development is to achieve driverless vehicles that can automatically cope with diverse tasks (e.g., lane keeping, lane change, and overtaking) [1]–[3]. Among the various tasks, overtaking is a difficult task because of the uncertain behavior of the surrounding vehicles [4]–[6]. Overtaking behaviors frequently occur in driving situations and are related to not only safety but also speediness. An autonomous vehicle is an integrated system consisting of five modules: localization, perception, decision-making, motion planning, and control [7], [8]. For overtaking, when driving, an autonomous vehicle needs to

The associate editor coordinating the review of this manuscript and approving it for publication was Kan Zheng.

make decisions on diverse driving motions with consideration for the surrounding environment. Decision-making, motion planning, and control modules are important for solving overtaking problems.

A variety of research has attempted to solve the overtaking decision-making problem. For overtaking decision problems, fuzzy logic has been utilized [9]–[11]. Fuzzy logic has the merit of considering various aspects of overtaking. However, these studies have only considered the ideal situation, where the surrounding vehicles are at a constant speed. Also, these studies have solved the problem of overtaking only one vehicle. Reinforcement learning has been employed to plan overtaking maneuvers [12], [13]. The algorithm has been trained on the overtaking problem through repeated simulation. The learned algorithm has shown good overtaking performance.

However, it is only verified by simulation, and the approach lacks verification of generality and safety.

Since overtaking is a complex maneuver, the various behaviors of the ego vehicle and surrounding vehicles should be considered to reflect reality beyond simulation. The motion planning algorithms for lane change have been researched in previous studies. Deterministic approaches have been utilized by formulating optimization problems [14, 15]. The approaches are simple and efficient, but could not consider diverse uncertainties which occur in lane change situations. A Markov Decision Process (MDP) and a Partially Observable Markov Decision Process (POMDP) have been employed to plan an optimal lane change policy [16]–[18]. MDP and POMDP are able to cope with uncertain system behaviors. However, these methods have problems in implementing these into a vehicle due to heavy computation loads.

Actual drivers usually drive in anticipation of the near future. The prediction is widely used for efficient decision-making and motion planning. Since appropriate prediction is helpful with low computational burden, diverse prediction methods have been utilized for autonomous driving applications. Deterministic prediction methods have been developed based on a fuzzy rule, finite-state machines, and various model buildings [19], [20]. Because deterministic prediction methods have limits, probabilistic prediction methods have been developed to augment robustness [21], [22]. Also, advanced probabilistic prediction algorithms have been devised utilizing data-driven approaches [23]–[25]. Inverse reinforcement learning has been employed to predict interactive motions considering discrete and continuous driving decisions [23]. The multi-modal probabilistic model could consider behavior intention based on deep neural networks [24]. Long short-term memory-based recurrent neural networks have been utilized for interactive prediction in multi-lane turn intersections [25]. Data-driven probabilistic prediction models considering interactive behavior are powerful in complex situations, such as ramp-merging, roundabout, and multi-lane turn intersections [23]–[25].

A model predictive control (MPC) framework constitutes an attractive method and is extensively utilized with the prediction. The MPC method employs a dynamic vehicle model to predict future states, and calculates an optimal control input trajectory sequence for tracking state reference while satisfying constraints [26], [27]. A robust MPC and a scenario MPC are used for an autonomous vehicle control algorithm [28], [29]. Although these MPC methods could increase robustness, they are too conservative or difficult to perform to be applied in all scenarios. A stochastic MPC (SMPC) has been described based on the chance-constraints optimization problem for autonomous driving [30], [31]. Previous studies have verified an autonomous driving algorithm adopting SMPC in only simulation and simple vehicle tests.

In this paper, we argue that it is crucial to pursue vehicle implementation as well as overtaking performance.

For vehicle implementation, it is important to consider efficient calculation and limitation of the vehicle. We propose efficient decision-making and motion planning based on probabilistic prediction and safety index. To improve safety within the near future, probabilistic predictions are employed that consider sensor noise, model uncertainty, and prediction uncertainty. An extended Kalman filter- (EKF) based probabilistic model is adopted in this paper. Learning-based probabilistic models show a powerful prediction performance. However, data-driven prediction models require heavier computation than the EKF-based model. Also, it is efficient to train on the data of the perception module that is actually used. Additionally, learning-based prediction techniques generally need historical information. This approach is vulnerable to effects such as object emergence, object disappearance, and false alarm, which frequently occur in perception modules of actual autonomous vehicles. A particle filter-based generic vehicle tracking framework could solve this problem [32]. However, this framework adds additional computation and needs to be tuned for the perception module to be used in this study. Since the target environment in this study is a simpler overtaking situation than ramp-merging, roundabouts, and intersections, the EKF-based prediction model was adopted in consideration of the trade-off relationship between calculation load and performance. Safety and driver acceptance is dealt with by employing a safety index based on human driving data.

Because all vehicles cannot be equipped with vehicle to vehicle (V2V) communications at present, autonomous vehicles should perceive the surrounding environment based on local sensors. Social perception has been devised to deal with local sensor limits [33], [34]. The perceived vehicle information could be used to infer the area beyond the blind spot or sensor limit. This approach enables rational behavior planning by inferring targets beyond perceived vehicles. It is powerful, especially in environments such as intersections and crosswalks. However, a vehicle that suddenly emerges outside the perception range is important in an overtaking situation. Also, inference for each perceived vehicle increases the calculation load, and social perception is affected by issues of the perception module. Therefore, a more efficient and feasible approach is required for the overtaking problem. In this paper, virtual targets are devised to cope with the limitation of cognitive range. The concept of a "virtual target" has been used as a virtual preceding vehicle for path following [35], [36]. This concept is adopted to solve the lane change problem in this study. Virtual targets are very efficient for vehicle implementation. Virtual targets do not burden the computation and are not affected by perception module issues.

In this paper, we present the autonomous overtaking algorithm containing decision-making, motion planning, and control modules. This study deals with issues for vehicle implementation such as cognitive range and computation load than existing relevant works. The main contribution of this study is to develop a simple, but performance guaranteed and

feasible overtaking algorithm. In the decision-making part, driving mode and target space are determined for the overtaking. The decision-making part is divided into three stages: availability, demand, and possibility of lane change. According to the driving mode, the appropriate motion is planned based on perceived vehicles and virtual targets. The SMPC calculates control input for tracking the desired motion. The proposed algorithm could achieve driver acceptance, efficient calculations, overcoming of perception limit, and consideration of diverse uncertainties. The performance of the proposed system has been investigated repeatedly through real-world driving tests in diverse lane change situations. The proposed algorithm is compared with the base algorithm through simulation. And, the performance of the proposed system has been investigated repeatedly through real-world driving tests.

II. PRELIMINARY

A. OVERTAKING SITUATION

To solve the overtaking problem, overtaking situations need to be defined. Figure 1 shows the traffic regulation about designated driving lanes in Korea, where the algorithm is actually implemented [37]. The driving lane is determined according to the type of vehicle. In any number of lanes, the first lane is the overtaking lane, and the second lane is the driving lane of the passenger vehicle. Since the algorithm is applied to a passenger vehicle in this study, the vehicle must drive on the first and second lanes. Therefore, the second lane is designated as a general driving lane, and the first lane is used only for overtaking. In this study, the first lane is named the overtaking lane and the second lane is named the driving lane.

	Four-Lane One-Way	Three-Lane One-Way	Two-Lane One-Way
1st Lane	Overtaking Lane	Overtaking Lane	Overtaking Lane
2nd Lane	Passenger Vehicles	Passenger Vehicles	All Vehicles
3rd Lane	Commercial Vehicles	Commercial Vehicles	
4th Lane	Special / construction vehicles		

FIGURE 1. Traffic regulation relevant to designated driving lanes in Korea.

Overtaking involves two lane-change maneuvers. One to enter the overtaking lane and another to return to the driving lane. In this study, the lane to be targeted for lane change is named the target lane. Therefore, in the case of entering the overtaking lane, the overtaking lane becomes the target lane. In the case of returning, the driving lane becomes the target lane. A vehicle to which the autonomous driving system is applied is termed an ego vehicle. For the safe overtaking behavior, the ego vehicle should check surrounding vehicles. The nearest forward vehicle on the current lane is called the preceding vehicle. Vehicles above the target lane are termed side vehicles. A pre-set target velocity of the ego vehicle is named as a set velocity (v_{set}). The set velocity is usually the speed limit of the road. The ego vehicle does not travel beyond the set velocity. When no vehicles are around, the ego vehicle travels at that velocity.

B. SAFE DISTANCE

The primary purpose of autonomous driving is to drive safely with surrounding vehicles. For this purpose, autonomous driving algorithms are designed with various safety indices. Various safety indices have been developed in previous studies, including clearance, time gap (TG), time to collision (TTC), warning index, and margin to collision (MTC) [38]. In this paper, a safe distance concept is adopted as a safety index. In defining safe distance, human driving data and collision avoidance performance are considered. Since overtaking is a complex maneuver that requires both lane keeping and lane change, different safe distances are used in lane keeping and lane change. In lane keeping situation, preceding and following vehicles could exist. Since safety for preceding vehicle is controllable by the ego vehicle, the preceding vehicle is important. In lane change situation, side vehicles are important. Figure 2 represents safe distances in lane keeping and lane change situations. The safe distances are derived by analyzing the driver data and combining various safety indices.
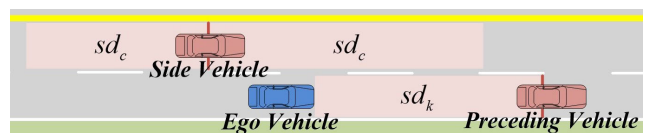
FIGURE 2. A concept of safe distance for safe motion planning with surrounding vehicles.

In lane-keeping situations, the ego vehicle needs to secure clearance of more than a certain distance from the preceding vehicle. A certain distance is defined as a safe distance (sd_k) in lane-keeping situations. sd_k could be well reflected by constant time-gap (CTG) and minimum clearance [39], [40]. Based on spacing policies of actual drivers in following a preceding vehicle, sd_k is defined as:

$$sd_k = v_e \times \tau_k + c_k. \tag{1}$$

where subscript e means the ego vehicle, v is the longitudinal velocity, τ_k is constant time-gap of lane-keeping, and c_k is a minimum clearance of lane-keeping. The parameters are adopted based on actual driver data [39].

In lane change situations, the ego vehicle plans lane change motion based on the distances from side vehicles. The distance is defined as a safe distance (sd_c) in lane change situations. The ego vehicle uses sd_c to determine the possibility of lane change or space to go for changing lane. Because the relative position between ego vehicle and the side vehicle is important in lane change situations, it is important to determine whether the side vehicle is located in front of or behind the ego vehicle. Also, the relative velocity between the ego vehicle and the side vehicle needs to be considered in lane change situations [41]. A larger distance is required when the velocity of the rear vehicle is faster than that of the

front vehicle. As a result, sd_c is designed as:

$$sd_c = \begin{cases} sd_{c1} & \text{if } x_s > 0 \\ sd_{c2} & \text{otherwise} \end{cases}$$

$$\text{s.t.} sd_{c1} = \max\left[(v_e - v_s), 0\right] \cdot \tau_{c1} + \max[v_e \cdot \tau_{c2}, c_c],$$

$$sd_{c2} = \max\left[(v_s - v_e), 0\right] \cdot \tau_{c1} + \max\left[v_s \cdot \tau_{c2}, c_c\right] \quad (2)$$

where subscript s means the vehicle on the side lane; x is the relative longitudinal position from the ego vehicle; τ_{c1} is the time gap for the relative velocity of lane change; τ_{c2} is the time gap for the minimum clearance of lane change; and c_c is the minimum clearance of lane change.

The parameters sd_c have been determined based on actual driver data. The relative distance with side vehicles has been analyzed in the lane change situation. Twelve drivers have collected lane change data while traveling 1500 km on six highways. The average age of drivers was 29.9 years, and 90% were male. All drivers have over 1 year of driving experience. For data accuracy, data collection was conducted in well-appointed roads on a clear day. Since setting the parameters as the mean value of the driving data is too conservative, the parameters are decided with a little margin from the boundary of the driving data. Also, kinematic analysis is conducted to consider both driver acceptance and collision avoidance.;

C. VIRTUAL TARGETS FOR PERCEPTION LIMIT

Since the current road is a mixed environment of normal vehicles and autonomous vehicles, all vehicles cannot be equipped with V2V. Therefore, autonomous vehicles perceive the surrounding environment based on local sensors. Inevitably, autonomous vehicles have a cognitive range limit. The perception range is influenced by blind spots as well as the sensor limits.

Figure 3 shows the cognitive range of limitations for two reasons. An autonomous vehicle recognized the surrounding environment. The autonomous vehicle was equipped with 2D-LiDARs and a LiDAR processor. The blue vehicle is an autonomous vehicle. Red points represent point clouds measured by LiDAR sensors. Red vehicles represent the surrounding vehicles recognized by the LiDAR processor. Although the point clouds of a vehicle 60 m ahead were detected, the perception module did not identify the vehicle
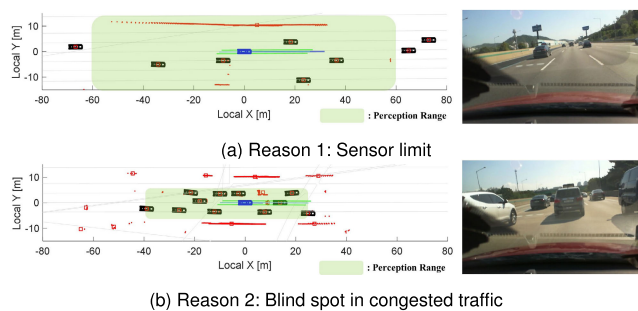

(a) Reason 1: Sensor limit

(b) Reason 2: Blind spot in congested traffic

FIGURE 3. Perception range limitation.

in Figure 3 (a). Therefore, the limit of the perception module to stably recognize vehicles was 60 m. Figure 3 (b) shows a situation in which the perception module cannot detect vehicles closer than 60 m. This is because of the blind spot caused by congested traffic.

In overtaking situations, interactions with side vehicles are important. When the ego vehicle conducts lane change, side vehicles might suddenly appear from outside of the perception range. In this study, the concept of virtual targets has been developed to cope with the limitation of cognitive range. The concept of virtual targets is shown in Figure 4. Since it is assumed that vehicles always exist at the perception limit, the virtual target can conduct decision-making and motion planning, considering the perception limit.
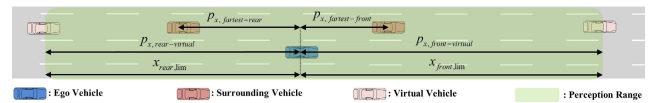

FIGURE 4. A concept of a virtual target for safe motion planning in an overtaking situation.

In the case of the open space, virtual targets are located on the sensor limit. In congested traffic, the virtual targets are located in front of and behind the recognized vehicles at the farthest distance. The velocity of the ego vehicle is used as a condition for distinguishing two cases. The threshold velocity is designed assuming that the vehicles travel with the general time gap (τ_k) in the recognition range [39]. The threshold velocity is as follows:

$$v_{vir,th} = (x_{rlim} + x_{flim})/\tau_k. \quad (3)$$

where subscript vir, th is the threshold for distinguishing the two cases; the subscript $rlim$ is the limit of rear sensor range (-60 m); and the subscript $flim$ is the limit of front sensor range (60 m).

The position of virtual targets is decided in two cases and is as follows:

$$x_{rvir} = \begin{cases} x_{rlim} & \text{if } v_e > v_{vir,th} \\ x_{rear} & \text{otherwise} \end{cases}$$

$$\text{s.t.} x_{rear} = \max[x_{rlim}, x_{rst} - \tau_k \cdot v_e] \quad (4)$$

$$x_{fvir} = \begin{cases} x_{flim} & \text{if } v_e > v_{vir,th} \\ x_{front} & \text{otherwise} \end{cases}$$

$$\text{s.t.} x_{front} = \max[x_{flim}, x_{fst} + \tau_k \cdot v_e] \quad (5)$$

where t represents the current time; subscript $rvir$ and $fvir$ mean rear (resp. front) virtual target; subscript rst and fst mean the rearmost (resp. the foremost) virtual target on the target lane.

Since it is risky to assume that a fast vehicle is in the rear and a slow vehicle is in front, the velocity of virtual targets is set as follows:

$$v_{rvir} = \min[v_{set}, v_e] \quad (6)$$

$$v_{fvir} = v_e \quad (7)$$

III. OVERALL ARCHITECTURE OF AUTONOMOUS DRIVING CONTROL ALGORITHM

The autonomous driving system is largely composed of five modules: localization, perception, decision-making, motion planning, and control [7], [8]. As shown in Figure 5, this study has focused on developing decision-making, motion planning, and control framework for overtaking maneuvers. The proposed algorithm is composed of four functional modules: prediction, driving mode decision, motion planning, and control. Each module operates sequentially, as shown in Figure 5. The proposed framework uses information from the upper processing modules: localization and perception. The localization module offers the position of the ego vehicle on the map. The localization module relies on the measurement from vision, around view monitor, differential GPS/INS platform, and HD map. The perception module provides the states of the surrounding obstacle. The perception module depends on six 2D-LiDARs and LiDAR processors. The perception system provides information on the type, relative position, speed, and direction of obstacles in all directions. V2X communication is excluded to avoid being constrained by infrastructure. The acquired information is processed by a LabVIEW/MATLAB-based motion planning PC and motion tracker based on Micro-autobox II. The system configuration of the test vehicle is shown in Figure 6.
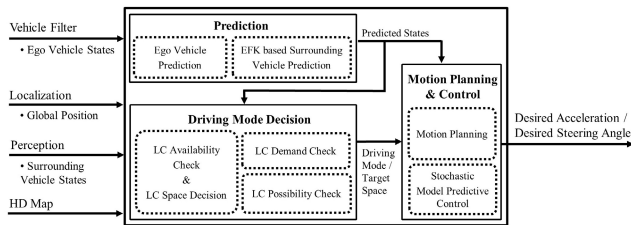

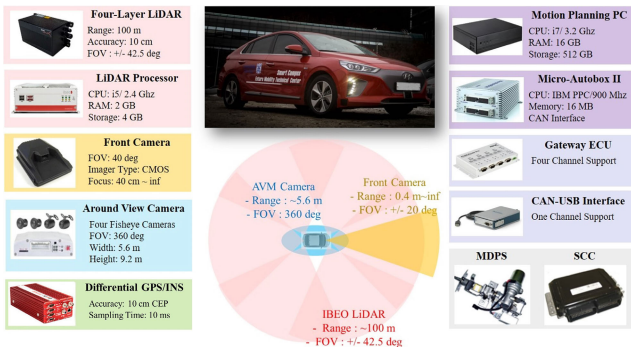**FIGURE 5.** The architecture of the proposed autonomous driving algorithm.

FIGURE 6. Vehicle configuration for implementation of the proposed algorithm.

A. VEHICLE MODEL

Since a vehicle is the controlled system plant for autonomous overtaking, the controlled model needs to reflect the real vehicle dynamic properties. There is a trade-off between simple and detailed models. The predictive control approach used in this study needs numerous optimization procedures. Therefore, decoupled control architecture is adopted in this paper. The decoupled control architecture has an advantage for computational efficiency.

The longitudinal dynamics model is designed to decide the desired longitudinal acceleration. Both the longitudinal dynamics and the actuator delay model are considered [42]. The state-space model of the longitudinal dynamics could be written as:

$$\dot{\bar{x}}_{lon} = A_{lon}\bar{x}_{lon} + B_{long}u_{lon}$$

$$\text{s.t.}\, A_{lon} = \begin{bmatrix} 0 & 1 & 0 \\ 0 & 0 & 1 \\ 0 & 0 & -1/\tau_a \end{bmatrix}, \quad B_{lon} = \begin{bmatrix} 0 \\ 0 \\ 1/\tau_a \end{bmatrix} \quad (8)$$

where, $\bar{x}_{lon} = [p\ v\ a]^T$ and $u_{lon} = a_{des}$ are state and input, respectively; a is longitudinal acceleration input, which is determined in the prediction time horizon by the control part; and τ_a represents the actuator delay of longitudinal acceleration.

The lateral dynamics model is designed by combining the bicycle model and error dynamics with a central path of the lane [43], [44]. Figure 5 presents the lateral dynamics model. The state-space model of the lateral dynamics could be written as:

$$\dot{\bar{x}}_{lat} = A_{lat}\bar{x}_{lat} + B_{lat}u_{lat} + F_{lat}\rho$$

$$\text{s.t.}\, A_{lat} = \begin{bmatrix} \dfrac{2C_f + 2C_r}{-mv} & \dfrac{2C_f l_f - 2C_r l_r}{-mv} & 0 & 0 \\ \dfrac{2C_f l_f - 2C_r l_r}{-I_z} & \dfrac{2C_f l_f^2 + 2C_r l_r^2}{-I_z v} & 0 & 0 \\ 0 & 1 & 0 & 0 \\ v & 0 & v & 0 \end{bmatrix},$$

$$B_{lat} = \begin{bmatrix} \dfrac{2C_f}{mv_x} \\ \dfrac{2C_f l_f}{I_z} \\ 0 \\ 0 \end{bmatrix}, \quad F_{lat} = \begin{bmatrix} 0 \\ 0 \\ -v_x \\ 0 \end{bmatrix} \quad (9)$$

where $\bar{x}_{lat} = \begin{bmatrix} \beta & \gamma & e_\psi & e_y \end{bmatrix}^T$, $u_{lat} = \delta_f$ and ρ denotes state, input, and disturbance, respectively; β is the tire-slip angle; γ is the yaw rate; e_ψ denotes the orientation error of the vehicle with respect to the center-line of the lane; e_y denotes the lateral position error with respect to the center-line of the lane; δ_f denotes the desired steering angle, which is determined in the prediction time horizon by the control part; ρ is the road curvature, C_f and C_r are stiffness coefficient of the front (resp. rear) tire, l_f and l_r are distances between the front (resp. rear) axle and the center of gravity, and m is an inertia of the vehicle around its yaw angle.

The tire stiffness is not constant because the overtaking maneuver requires high speed lane changing. Since the driving range of this study is mild driving ($a_y < 0.2g$), a steady-state tire model is appropriate. Lateral tire force is in the linear tire region. In this context, the lateral tire stiffness is almost unchanged, so the effect on variable speed could be neglected.

Dynamic parameters are set as nominal values provided by the manufacturer of the tested vehicle.

B. PREDICTION MODEL

The appropriate prediction contributes to decision-making, motion planning, and control of autonomous driving. To enhance safety, given the potential behavior of surrounding vehicles, it is essential to predict the ego vehicle and the surrounding vehicles. The prediction model used in this paper is shown in Figure 7.
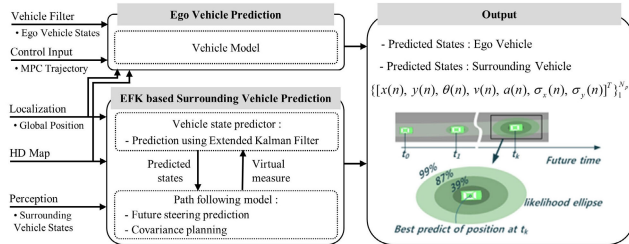

FIGURE 7. Architecture of probabilistic prediction.

For the prediction of the ego vehicle, the decoupled vehicle model is applied to the control input trajectory calculated by MPC. The predicted model of the ego vehicle is discretized as:

$$\bar{x}_{lon}(n+1) = A_{lon}\bar{x}_{lon}(n) + B_{lon}u_{lon}(n)$$
$$\bar{x}_{lat}(n+1) = A_{lat}(n)\bar{x}_{lat}(n)$$
$$+ B_{lat}(n)u_{lat}(n) + F_{lat}\rho \quad (10)$$

where n is the prediction step. The prediction horizon is 2 s, and the prediction sampling time (t_{sam}) is 0.1 s. This means that the prediction sample is 20 ($n = 0, \ldots, 19$).

A probabilistic prediction model is adopted for the prediction of the surrounding vehicles. The prediction model is based on the probabilistic movement characteristics of the surrounding vehicles. In a vehicle state predictor, the vehicle's reasonable position and its error covariance are predicted by EKF using the desired yaw rate generated by the path-following model as the virtual measurement [22]. Therefore, the error covariance is propagated according to the prediction step by EKF. The initial covariance matrix used in the prediction utilizes the covariance matrix of the estimation result. The final outputs from the probabilistic prediction model are shown in Figure 8 and as follows: the relative longitudinal position from ego vehicle (x), the relative lateral position from ego vehicle (y), the yaw angle (θ), the longitudinal velocity (v), the longitudinal acceleration (a), the longitudinal position standard deviation (σ_x), and the lateral position standard deviation (σ_y).

There are probabilistic prediction methods that could perform better than EKF-based prediction [23]–[25], [45]. However, in this paper, the EKF-based probabilistic prediction model is adopted in consideration of vehicle implementation. The computation power is important for the algorithm

implementation of the vehicle. Figure 8 shows the calculation time of the EKF-based prediction model. The total data included 6574 steps. The relative value is important because the absolute value of the computation time depends on the CPU performance. As the number of vehicles to be predicted increases, the calculation time increases. The calculation time of the EKF-based model is compared with other data-driven prediction models. These predictors were learned from the data of the perception module used in this paper [25], [45]. One is the RNN-based method, which predicts behavior through the accumulated trajectory of the target vehicle [25]. The other is a predictor, which combines RNN and EKF methods to reduce the computational load [45]. The predictor determines the target lane of the vehicle through the accumulated trajectory and predicts behavior to the target lane-based EKF method. Figure 9 shows the relative computational ratio of the two models over the EKF-based model. Both techniques need about 480- and 60-times more computation than the EKF-based model, respectively. Heavy computation makes implementation difficult because overtaking requires predicting multiple vehicles.
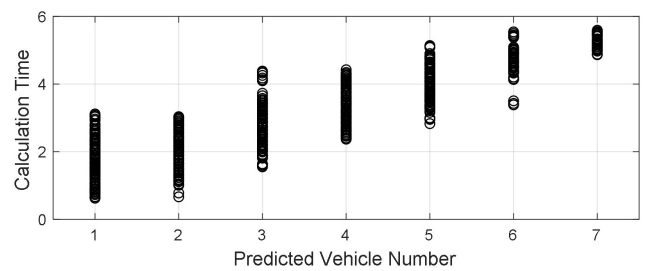

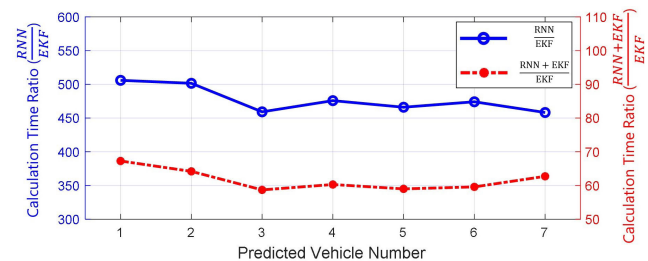**FIGURE 8.** Calculation time of EKF-based prediction model.

FIGURE 9. Calculation time comparison of data-driven models and EKF-based model.

IV. DRIVING MODE DECISION FOR OVERTAKING

Advanced overtaking requires active lane change, not passive lane change [41]. For active lane-change maneuver, three driving modes are devised: lane-keeping mode (LK); lane change mode (LC); and lane-keeping mode for lane change (LKC). Figure 10 shows a flow chart of the driving mode decision. During lane-keeping mode, the ego vehicle follows v_{set} or a preceding vehicle. A lane change is necessary when entering to an overtaking lane or returning to a driving lane based on the states of surrounding vehicles. For overtaking
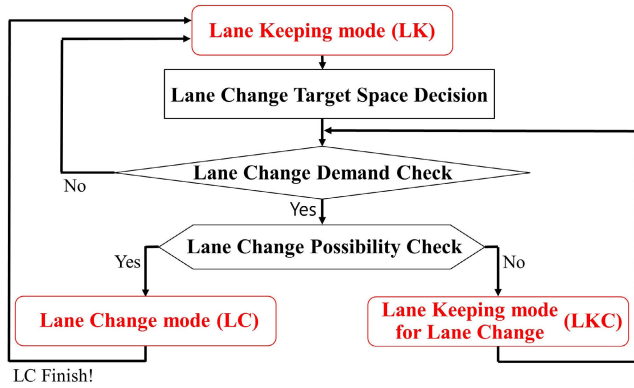
FIGURE 10. Flow chart of driving mode decision for overtaking.

decisions, three concepts about lane change are developed: target space, demand, and possibility. After checking three concepts, the driving mode is determined.

A. LANE CHANGE TARGET SPACE DECISION

The first step in determining the driving mode for lane changes is to check the condition of side vehicles on the target lane. A concept of 'target space' has been developed in this paper. Target space means the space to enter for lane change between the vehicles on the target lane. Before deciding the target space, candidates of the target space are identified. As shown in Figure 11, space candidates for lane changes could be yielded by applying sd_c to the virtual targets and detected vehicles in the target lane. One side vehicle makes two space candidates. Each space candidate has a 'j' index. The states of each space, such as its position and velocity, depend on the states of the vehicle that created it. Since the ego vehicle could accelerate and decelerate for the active lane change, the diverse behaviors of the ego vehicle need to be assumed to find the optimal space for a lane change. It is assumed that the ego vehicle has several acceleration candidates. The minimum value of the acceleration candidates is constant. The maximum value of the acceleration candidates is varied depending on a preceding vehicle. Several acceleration candidates are derived between the maximum and minimum acceleration. The assumed behavior of the ego vehicle is predicted according to acceleration candidates. The assumed behavior is expressed as follows:

$$v_i(n+1) = v_i(n) + a_i(n) \times t_{sam}$$
$$p_i(n+1) = p_i(n) + v_i(n) \times t_{sam} \qquad (11)$$

where subscript i is the i-th acceleration candidate.

A target space shall be decided among space candidates. Two conditions are used for determining the target space. These conditions are derived by the decision rule of human drivers in the lane-change maneuver. Drivers do not intend to enter a space that is too far or too narrow for a lane change. The first condition is the time that the ego vehicle arrives at space. The second condition is the clearance between consecutive space candidates. An optimization problem is formulated to decide the target space. The space candidate, which has the lowest cost, is selected as the target space. The optimization problem is as follows:

$$\min_{i,j} J_{ij} = T_{ij}/C_j$$
$$\text{s.t. } T_{ij} = p_{ij}/v_{ij},$$
$$p_{ij} = \sum_{n=1}^{N_p} (p_j(n) - p_i(n) \pm sd_{c,ij}(n))/N_p,$$
$$v_{ij} = \sum_{n=1}^{N_p} (v_j(n) - v_i(n))/N_p,$$
$$C_j = \sum_{n=1}^{N_p} (p_{j+1}(n) - p_j(n))/N_p \qquad (12)$$

where J means the optimization cost; subscript j is the j-th space candidate; T denotes the time for arriving at the space candidates; N_p is maximum prediction step and C denotes the clearance between the consecutive space candidates.

B. LANE CHANGE DEMAND CHECK

To determine whether overtaking proceeds, it is important to decide what information in the adjacent lane will be used. Previous studies have utilized traffic flow for the overtaking decision. In previous research, traffic flow is characterized by microscopic and macroscopic points of view [46]. Since local sensors of the ego vehicle could only measure a limited area, the microscopic point of view has been utilized in overtaking decisions [31]. In an ideal situation, it is reasonable to use the traffic flow for overtaking decisions. However, side vehicles drive with various velocity on a real road. When drivers decide to overtake, they judge based on the velocity of the space they are going to go, rather than the average velocity of the target lane. Therefore, in this study, the target space defined above is used for overtaking decisions. The decision algorithm utilizes the velocity of the vehicle in front of the target space. The velocity is named as a target space velocity
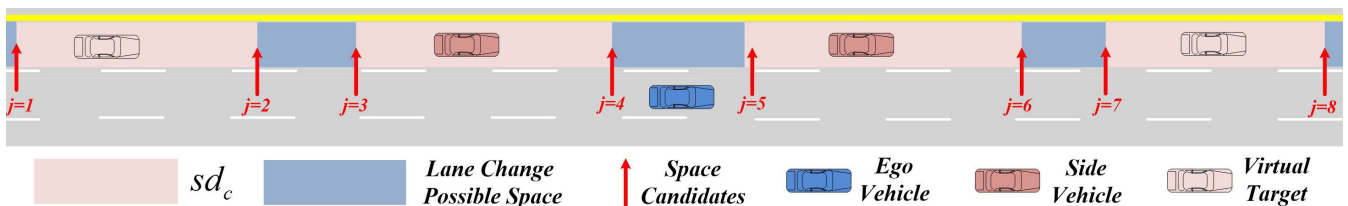

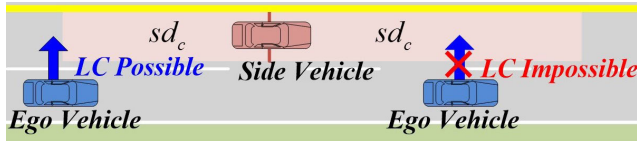**FIGURE 11.** Space candidates for lane change based on sd_c.

FIGURE 12. A concept of lane change possibility based on safe distance.

FIGURE 13. Desired position planning in LKC mode.

(v_{space}). Lane change is demanded by comparing v_{space} with the velocity of the preceding vehicle (v_{prc}).

When overtaking, it is necessary to change lane twice. Once when the ego vehicle meets a slow preceding vehicle. In this case, lane change is demanded to overtaking lanes. Another is when the ego vehicle returns from the overtaking lane to the driving lane. In this case, lane change is demanded of driving lanes. Therefore, different conditions are needed for two reasons. The enter (to the overtaking lane) condition, which is defined as:

$$v_{prc} < v_{set} \land v_{prc} < v_{space} \tag{13}$$

The return (to the driving lane) condition is defined as follows:

$$v_{set} \le v_{space} \lor v_{prc} < v_{x,space} \tag{14}$$

C. LANE CHANGE POSSIBILITY CHECK

When a lane change is demanded, the driving mode changes from LK mode to LKC mode or LC mode. To decide which mode to proceed between LKC mode and LC mode, the ego vehicle needs to judge a possibility of the lane change based on sd_c of side vehicles. If any side vehicle is situated closer than sd_c, the lane change is impossible. Figure 12 shows a concept of the lane change possibility. When relative positions of side vehicles are bigger than the sd_c of each vehicle in the all prediction horizon, a lane change is possible. The LC mode is started when a lane change is possible. Even during the lane change mode, the lane change possibility is continuously checked. The possibility has been checked until the ego vehicle crosses the lane. The condition of the lane change possibility is given by:

$$|p_{ms}| > |sd_{c,ms}| \tag{15}$$

where subscript ms means the ms-th side vehicles on target lane ($m = 1, \ldots, N_{ms}$); and N_{ms} means the number of side vehicles.

The condition is checked in all prediction horizons for all side vehicles detected on the target lane. LC mode does not start if any condition is not met about all checks. LKC mode continues in this case.

V. MOTION PLANNING AND CONTROL

Desired motion is planned according to the driving mode decided above. In motion planning, desired states are determined. For tracking planned motion, a SMPC is utilized [31]. Solver FORCES is used to solve the problem of SMPC [47]. The solver is operated in MATLAB. Since the distributed
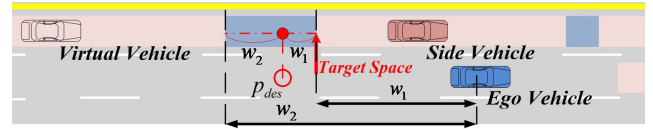
vehicle model is used, motion planning and control are also divided into longitudinal and lateral motions.

A. LONGITUDINAL MOTION PLANNING AND CONTROL

In longitudinal motion planning, velocity and position are used as desired states and are as follows:

$$\bar{x}_{lon,des} = \begin{bmatrix} p_{des} & v_{des} & 0 \end{bmatrix}^T \tag{16}$$

where subscript *des* denotes the desired states.

When the calculated v_{des} is greater than v_{set}, v_{des} is determined as v_{set}.

In LK mode, the desired states are determined by a preceding vehicle in the current lane. The desired velocity is decided as the set velocity or the velocity of a preceding vehicle. It is inefficient to follow the velocity of the preceding vehicle identically when the preceding vehicle is too far away. Therefore, the distance to the preceding vehicle affects the desired velocity. The desired position is set to prevent a rear collision when a preceding vehicle is closer than sd_k. This could be the case when a side vehicle cuts-in. In LK mode, the desired states are expressed as:

$$v_{des} = \begin{cases} v_{prc}, & \text{if } p_{prc} < sd_{k,prc} \\ v_{safe}, & \text{otherwise} \end{cases} \tag{17}$$
$$\text{s.t.} v_{safe} = \alpha \cdot v_{set} + (1 - \alpha) \cdot v_{prc},$$
$$\alpha = \frac{p_{prc} - sd_{k,prc}}{p_{prc}}$$
$$p_{des} = \min[0, p_{safe}]$$
$$\text{s.t.} p_{safe} = p_{prc} - sd_{k,prc} \tag{18}$$

In LCK mode, the target space is important to decide the desired states. Also, the preceding vehicle is considered. The desired velocity is determined with v_{space} and v_{prc}. The desired position is also determined as an internecine point by the sd_c of the consecutive vehicles in the target space. Figure 13 represents desired position planning in the LKC mode. In the LKC mode, the desired states are expressed as:

$$v_{des} = \min[v_{prc}, v_{space}] \tag{19}$$
$$p_{des} = \min[p_{safe1}, p_{safe2}]$$
$$\text{s.t.} p_{safe1} = p_{prc} - sd_{k,prc},$$
$$p_{safe2} = \frac{w_2(p_{spf} - sd_{c,spf}) + w_1(p_{spr} + sd_{c,spr})}{w_1 + w_2},$$
$$w_1 = |p_{spf} - sd_{c,spf}|,$$
$$w_2 = |p_{spr} + sd_{c,spr}| \tag{20}$$

where subscript *spf* means the vehicle in front of target space; and subscript *spr* means the vehicle behind target space.

In the LC mode, it is important to determine whether the ego vehicle crosses the lane. Before crossing the lane, the ego vehicle has desired states of LCK mode. After crossing the lane, the ego vehicle has desired states of LK mode. At this time, the nearest vehicle on the newly entered lane becomes a preceding vehicle.

The SMPC problem is presented to calculate the desired longitudinal acceleration. The SMPC problem is formulated with the vehicle dynamics model, reference, constraints, and input limit. Repeating at each time step, the solving process of the optimization problem is formulated as follows:

$$\min \sum_{n=0}^{N_p-1} \mathbb{E}\left(\|\tilde{x}_{lon}(n+1)\|^2_{\mathbf{Q}_{lon}} + \|u_{lon}(n)\|^2_{\mathbf{R}_{lon}}\right)$$
$$\text{s.t. } \bar{x}_{lon}(n+1) = A_{lon}(n)\bar{x}_{lon}(n) + B_{lon}(n)u_{lon}(n),$$
$$\Pr\left(g_{lon}^T(n+1)\bar{x}_{lon}(n+1) \le \bar{x}_{lon,bound}(n+1)\right)$$
$$\ge 1 - \varepsilon_{lon}(n),$$
$$g_{lon} = \begin{bmatrix} 1 & 0 & 0 \\ -1 & 0 & 0 \end{bmatrix}^T,$$
$$u_{lon,\min} \le u_{lon}(n) \le u_{lon,\max},$$
$$(n = 0, \ldots, N_p - 1) \qquad (21)$$

where $\tilde{x} = \bar{x}_{lon,des} - \bar{x}_{lon}$; Q_{lon} is and R_{lon} is the state and input weighting matrix of longitudinal states. $\bar{x}_{lon}(n)$ is the predicted longitudinal states of ego vehicle at time t+n derived by applying the control sequence u_{lon} to the longitudinal model Eq. (8) with initial condition $\bar{x}_{lon}(0) = \bar{x}_{lon}(t)$. g_{lon} and $x_{lon,bound}$ are related to a longitudinal safe driving envelope, which is defined to guarantee collision avoidance. Boundary ($x_{lon,bound}$) for the safe driving envelope is defined as the longitudinal position to surrounding vehicles. ε_{lon} is the longitudinal risk parameter, which is related to a chance constraint to be satisfied with a specified probability. $u_{lon,\min}$ and $u_{lon,\max}$ denote longitudinal control input constraints. The details of parameters and constraints about SMPC are given in [31].

B. LATERAL MOTION PLANNING AND CONTROL
In lateral motion planning, yaw rate, and lateral position are used as desired states. Yaw rate could be represented as a lateral position. Desired states of sideslip angle and yaw angle are always zero, which improves stability. Therefore, the only lateral position is the target of motion planning. Desired states of lateral motion are followed:

$$\bar{x}_{lat,des} = \begin{bmatrix} 0 & \gamma_{des} & e_{y,des} & 0 \end{bmatrix}^T$$
$$= \begin{bmatrix} 0 & \frac{\ddot{e}_{y,des}}{v_x} & e_{y,des} & 0 \end{bmatrix}^T \qquad (22)$$

In LK mode or LKC mode, the desired lateral position is defined as zero, which means that the vehicle tracks the centerline. In the LC mode, the desired lateral position is defined as the hyperbolic tangent path. This desired position reflects the lane change and has a low acceleration jerk [31].

In LC mode, the desired lateral position could be given by:

$$e_{y,des} = \begin{cases} e_{y,LC}, & \text{if LC mode} \\ 0, & \text{otherwise} \end{cases}$$
$$\text{s.t.} e_{y,LC} = C_1 \cdot \tanh(C_2 \cdot k + C_4) + C_3 + e_{y,0}$$
$$C_1 = \frac{\pm W - e_y}{2}, C_2 = \sqrt{\frac{\pm a_{y,\lim}}{a_y \cdot C_1}}$$
$$C_3 = -\frac{t_{LC}}{2}C_2, C_4 = \frac{\pm W - e_y}{2}$$
$$t_{LC} = \frac{2}{C_2}\tanh^{-1}\frac{W - C_4 - e_y}{C_1} \qquad (23)$$

where subscript $a_{y,lim}$ is the lateral acceleration limit; W is the road width; and t_{LC} is the lane change time.

The SMPC problem is presented to calculate the desired steering angle. The SMPC problem is formulated considering the vehicle dynamics model, reference, constraints, and input limit. Repeating at each time step, the solving process of the optimization problem is formulated as follows:

$$\min \sum_{n=0}^{N_p-1} \mathbb{E}\left(\|\tilde{x}_{lat}(n+1)\|^2_{\mathbf{Q}_{lat}} + \|u_{lat}(n)\|^2_{\mathbf{R}_{lat}}\right)$$
$$\text{s.t. } \bar{x}_{lat}(n+1) = A_{lat}(n)\bar{x}_{lat}(n) + B_{lat}(n)u_{lat}(n)$$
$$+ F_{lat}(n)\rho,$$
$$\Pr\left(g_{lat}^T(n+1)\bar{x}_{lat}(n+1) \le \bar{x}_{lat,bound}(n+1)\right)$$
$$\ge 1 - \varepsilon_{lat}(n),$$
$$g_{lat} = \begin{bmatrix} 0 & 0 & 0 & 1 \\ 0 & 0 & 0 & -1 \end{bmatrix}^T,$$
$$u_{lat,\min} \le u_{lat}(n) \le u_{lat,\max},$$
$$(n = 0, \ldots, N_p - 1) \qquad (24)$$

where $\tilde{x} = \bar{x}_{lat,des} - \bar{x}_{lat}$; Q_{lat} is and R_{lat} is the state and input weighting matrix of longitudinal states; $\bar{x}_{lat}(n)$ is the predicted lateral states of ego vehicle at time t+n derived by applying the control sequence u_{lat} to the lateral model Eq. (9) with initial condition $\bar{x}_{lat}(0) = \bar{x}_{lat}(t)$. g_{lat} and $x_{lat,bound}$ are related with a lateral safe driving envelope which is defined to guarantee collision avoidance and lane departure. Boundary ($x_{lat,bound}$) for the safe driving envelope is defined as the lateral position to surrounding vehicles and lane information. ε_{lat} is the lateral risk parameter which is related with a chance constraint to be satisfied with a specified probability. $u_{lat,\min}$ and $u_{lat,\max}$ denote lateral control input constraints. The details of parameters and constraints about SMPC are in [31].

VI. EVALUATION RESULTS
A. SIMULATION RESULTS
The proposed overtaking algorithm has been evaluated through simulation. The simulation environment is a two-lane straight road. Figure 14 and Table 1 represent the initial condition of ego vehicle and surrounding vehicles. Seven surrounding vehicles were placed in arbitrary positions. Surrounding vehicles use the initial velocity as the set velocity

FIGURE 14. The initial condition of the simulation.

TABLE 1. The initial condition of the simulation.

Vehicle	X position [m]	Y position [m]	Velocity[km/h]
Ego	0	0	100
Target 1	-70	3.5	110
Target 2	-30	3.5	100
Target 3	10	3.5	100
Target 4	68	3.5	90
Target 5	70	0	80
Target 6	110	0	80
Target 7	120	3.5	100

and proceeds to safety control if a preceding vehicle exists. The time gap used for safety control is 1.36 s [39]. The surrounding vehicles do not change lanes. Vehicle model used in the simulation has input constraints described in SMPC problems. To show the effectiveness of virtual targets, an algorithm without a virtual target has been compared with the proposed algorithm (with the virtual target).

Figure 15 shows the simulation results. At two seconds, both algorithms demand the lane change to the overtaking lane because of the slower preceding vehicle. Then no virtual algorithm tries to enter in front of target 3. However, as target 4 is recognized in the perception range, it changes to enter the space between targets 2 and 3. This could be seen through the fluctuating desired position, desired velocity, and acceleration. On the other hand, the proposed algorithm attempts to enter the space between targets 2 and 3 as soon as a lane change is required. This is because the proposed algorithm always thinks virtual targets are placed on the perception range limit. The proposed algorithm could prepare for vehicles coming in outside the perception range. As a result, the proposed algorithm enters the overtaking lane more quickly. Then, it overtakes targets 5 and 6 and returns to the driving lane again. The proposed algorithm travels a greater distance with a smoother acceleration than no virtual algorithm.

B. VEHICLE TEST RESULTS

The proposed lane change algorithm has been evaluated through a real vehicle test. The test vehicle is introduced in Section 3. The test environment is the Gyeongbu Expressway in Korea. The highway is four lanes one way and has a speed limit of 110 km/h. The vehicle test has been conducted using the first and second lanes according to the road regulations. The total driving distance was 200 km and 106 lane changes were made for overtaking. Figure 16 shows the snapshots of the selected one overtaking situation among the 106 lane-change maneuvers. The selected overtaking situation is a situation in which the ego vehicle enters to the overtaking lane after seeing a slow preceding vehicle. And because of slow vehicles in the driving lane, the ego vehicle continues

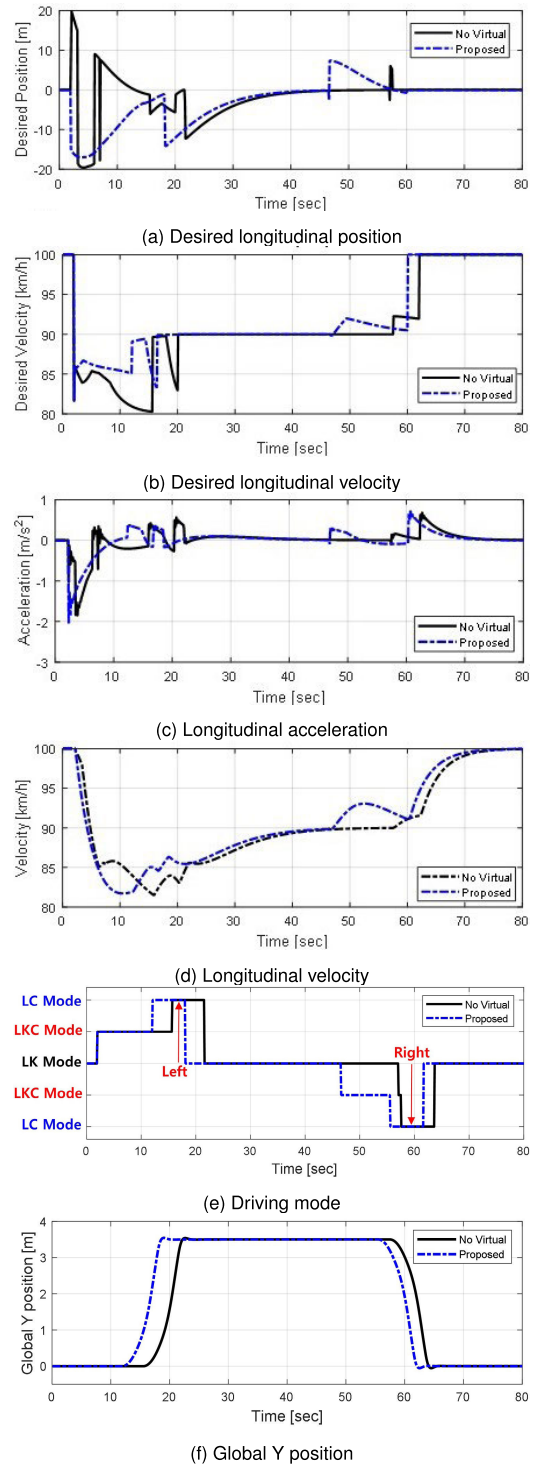**FIGURE 15.** Simulation results.

to drive in the overtaking lane. Then, the ego vehicle returns to the proper space in the driving lane. As a result, the ego vehicle overtakes four vehicles. In the snapshots, the blue vehicle is the ego vehicle. The black vehicles are surrounding vehicles. Important vehicles among surrounding vehicles are colored vehicles. The red vehicle is the preceding vehicle.
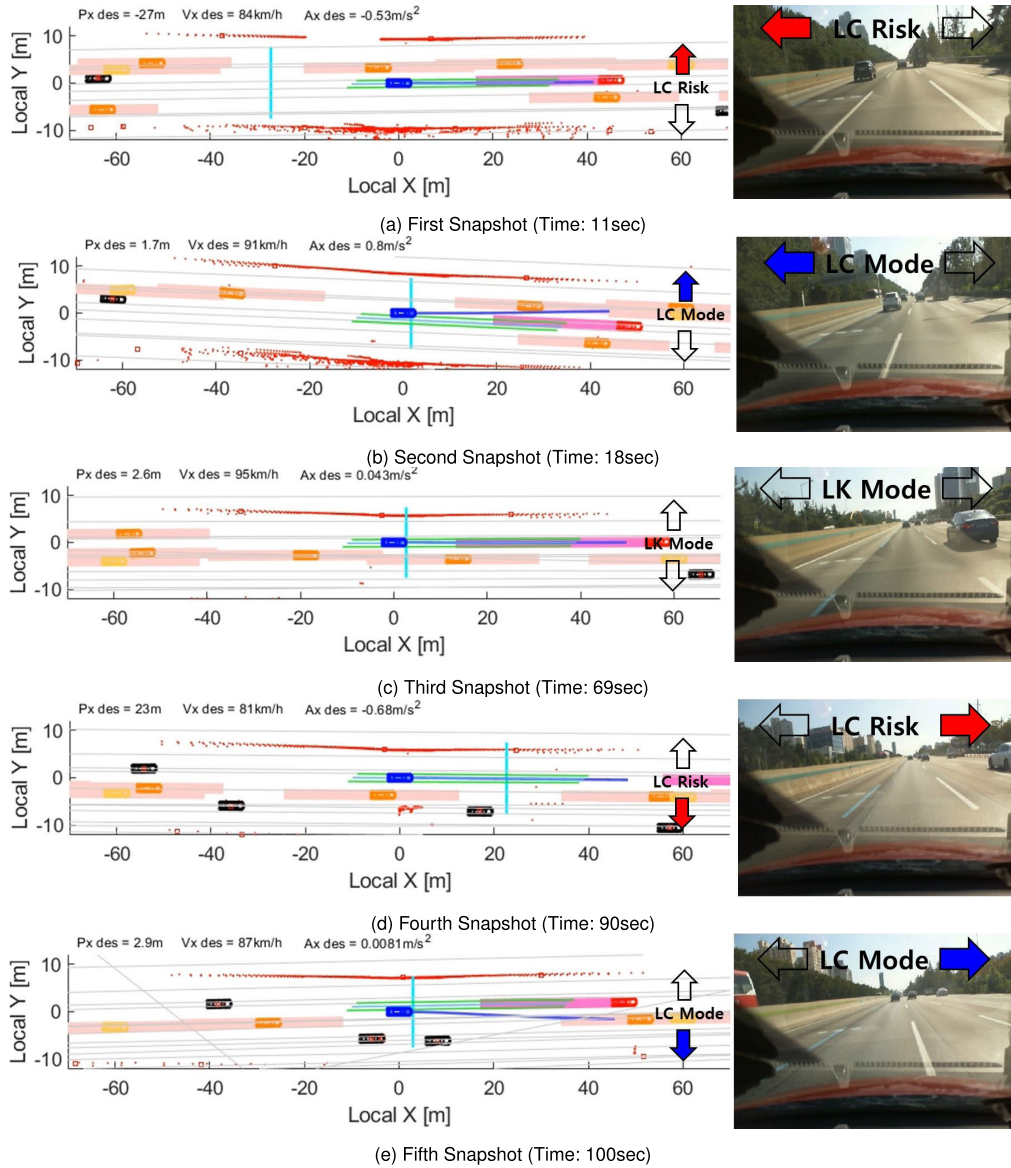
(a) First Snapshot (Time: 11sec)

(b) Second Snapshot (Time: 18sec)

(c) Third Snapshot (Time: 69sec)

(d) Fourth Snapshot (Time: 90sec)

(e) Fifth Snapshot (Time: 100sec)

FIGURE 16. Vehicle test snapshots: the selected one overtaking situation.

The orange vehicles are vehicles on side lanes. The boxes drawn around important vehicles indicate safe distances. The red points represent point clouds of the LiDAR sensors. The blue line means the desired path of the ego vehicle. The green lines represent the lanes recognized by the camera sensor. The azure line means the reference of a longitudinal position. It could be seen that the reference changes according to the decided target space. In this paper, the driving mode is very important. The concepts of lane change demand, and possibility are expressed by arrows. The arrow represents the driving mode and the direction of the lane change. The colored arrows indicate the lane change demand. A red arrow represents that the lane change is impossible. A blue arrow indicates that the lane change mode proceeds because the safe distances have been sufficiently guaranteed. The texts at the top of the snapshot represent the reference position, the reference velocity, and the desired acceleration, respectively.

Figure 17 represents the test results of the selected over-taking situation: driving mode, overtaking decision velocity, distance with surrounding vehicles, safety domain with surrounding vehicles, acceleration, and lateral position. These figures show that the ego vehicle proceeds to overtake, while using appropriate acceleration and maintaining safety with the surrounding vehicles. Figure 17 (a) indicates the driving mode that is related to the lane change demand and possibility concept for the overtaking. The left lane change is for entering to the overtaking lane, and the right lane change is for returning to the driving lane. In Figure 17 (b), the overtaking decision velocities are shown. The lane change demand is determined according to the decision velocities.
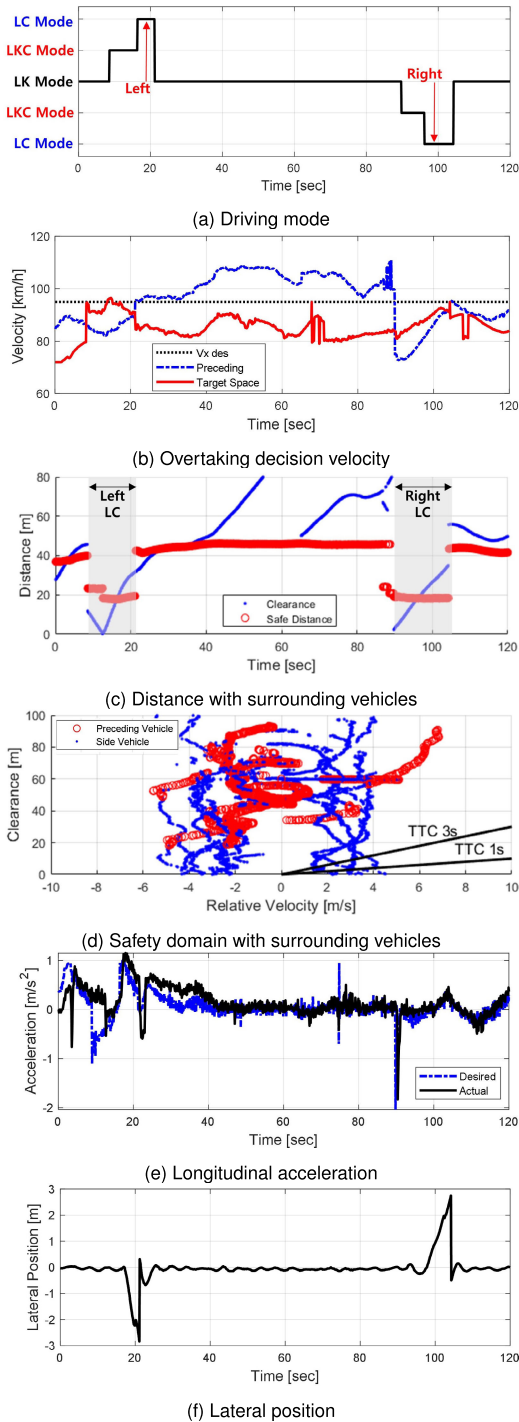
(a) Driving mode

(b) Overtaking decision velocity

(c) Distance with surrounding vehicles

(d) Safety domain with surrounding vehicles

(e) Longitudinal acceleration

(f) Lateral position

FIGURE 17. Vehicle test results: the selected one overtaking situation.

In Figure 17 (c), the distances with the surrounding vehicle are indicated as clearance and safe distance. The gray area in Figure 17 (c) indicates the situation where the lane change is demanded. In the grayed out area of Figure 17 (c), the states of the nearest vehicle on the target lane are displayed. In other areas, the states of the preceding vehicle are displayed. When the clearance is greater than the safe distance in the gray

area, lane change mode starts. This shows the concept of lane change possibility. In the case where lane change is not demanded, the lane-keeping situation shows the clearance and the safe distance from the preceding vehicle. It shows that the distance to the preceding vehicle is above the safe distance. The clearance control characteristics described in Figure 17 (d) show that the behaviors of the ego vehicle are in a safe region with a sufficient safety margin. The acceleration in Figure 17 (e) is satisfactory for both smooth ride quality and clearance control. Figure 17 (f) indicates the lane change moment and shows that the lateral position has a sudden change within a very short time.

Figure 18 shows cumulative test data was about 106 lane changes. In Figure 18 (a), (b), and (c), the ego vehicle always maintains safety performance with a preceding vehicle. The
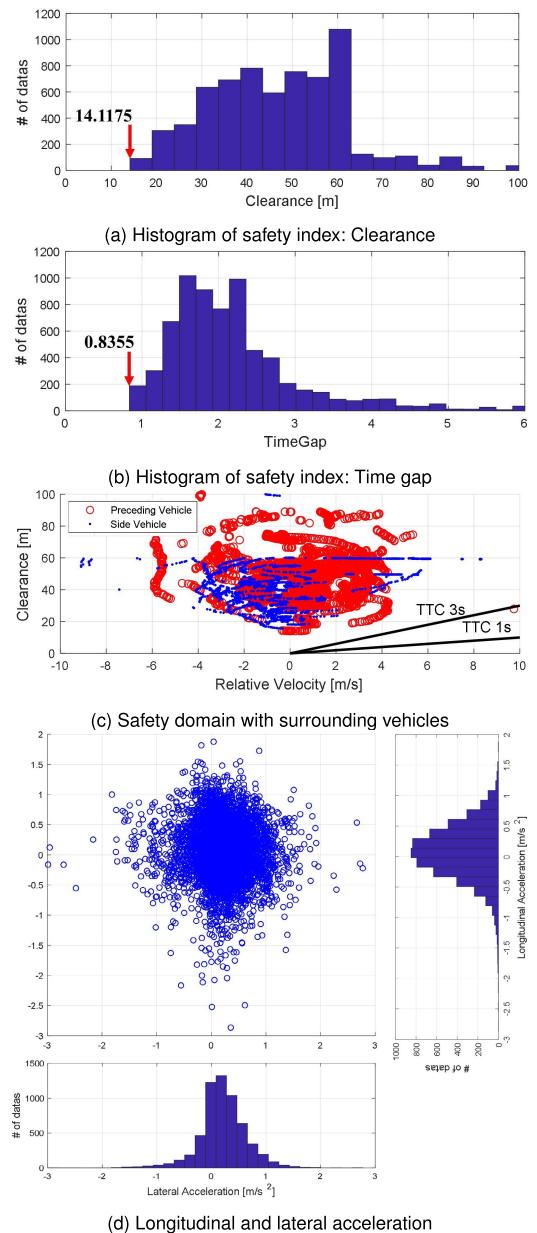

(a) Histogram of safety index: Clearance

(b) Histogram of safety index: Time gap

(c) Safety domain with surrounding vehicles

(d) Longitudinal and lateral acceleration

FIGURE 18. Vehicle test results: cumulative test data.

minimum clearance is 14.1175 m, and the minimum time gap is 0.8355 s. This means that safety performance is maintained within the defined safe distances. All lane changes have been carried out while keeping the safety of the surrounding vehicles. Lastly, figure 18 (d) represents the longitudinal and lateral acceleration of the ego vehicle during 106 lane changes. This indicates that overtaking maneuvers have been performed without compromising the ride quality of passengers.

VII. CONCLUSION

Here we describe a novel, virtual, target-based overtaking algorithm. The overtaking situation has been defined by the regulation analysis. For driver acceptance and safety with the surrounding vehicles, safe distances have been devised based on existing safety indices and human driving data. Since most autonomous vehicles recognize the environment by the local sensor, there is a problem with the limitation of the cognitive range. Virtual targets have been devised to cope with this problem. This paper focuses on decision-making, motion planning, and control among various autonomous driving functions. Because proper prediction is helpful for focused functions, the probabilistic prediction model is presented to deal with diverse uncertainties. Decision-making and motion planning have been designed based on the probabilistic prediction-based safe distance, which can achieve safety performance without a heavy computational burden. The algorithm has considered the decision rules that drivers adopt when overtaking. For this purpose, the concepts of target space, demand, and possibility for lane change have been devised. The desired driving mode is decided to handle overtaking. Intuitive and efficient motion planning has determined desired states and constraints according to the desired driving mode. Finally, the SMPC has been used to track the desired motion. The performance of the proposed algorithm has been investigated via simulation studies and vehicle tests on highways. The simulation results show the advantage of virtual targets. The vehicle test results reveal that our autonomous vehicle quickly overtakes the surrounding vehicles in accordance with traffic regulations. Safe and comfortable overtaking maneuvers have been achieved due to the consideration of vehicles appearing outside the sensor range.

The main contributions of this work are as follows: 1) the virtual vehicle is devised to overcome perception limitation by local sensors and blind spots; 2) the safe distance is defined for driver acceptance and safety with surrounding vehicles; 3) the efficient and intuitive decision-making and motion planning are achieved using driving mode and target space; 4) based on probabilistic prediction and SMPC, the smooth and safe driving performance are accomplished with light computation for vehicle implementation; and 5) the efficacy of virtual target and repetitive driving performance are confirmed by simulation and actual vehicle test.

Future works aim at advancing the proposed algorithm, which could perform successful lane changes in congested traffic. In congested traffic, it is necessary to transmit the intent of the lane change. The intent could be conveyed to surrounding vehicles through turn signal or lateral motion of the ego vehicle. It is also important to infer the intention of yield from nearby vehicles. The proposed algorithm could be improved to carry out interactive lane changes. Future works should also thoroughly test advanced interactive lane changes on actual roads.

REFERENCES

[1] A. Broggi, *Automatic vehicle guidance: The experience of the ARGO autonomous vehicle*. Singapore: World Scientific, 1999.
[2] J. P. How, B. Behihke, A. Frank, D. Dale, and J. Vian, "Real-time indoor autonomous vehicle test environment," *IEEE Control Syst. Mag.*, vol. 28, no. 2, pp. 51–64, Apr. 2008.
[3] C. Urmson and W. Whittaker, "Self-driving cars and the urban challenge," *IEEE Intell. Syst.*, vol. 23, no. 2, pp. 66–68, Mar. 2008.
[4] T. Shamir, "How should an autonomous vehicle overtake a slower moving vehicle: Design and analysis of an optimal trajectory," *IEEE Trans. Autom. Control*, vol. 49, no. 4, pp. 607–610, Apr. 2004.
[5] F. Wang, M. Yang, and R. Yang, "Conflict-probability-estimation-based overtaking for intelligent vehicles," *IEEE Trans. Intell. Transp. Syst.*, vol. 10, no. 2, pp. 366–370, Jun. 2009.
[6] Y. Zhu, D. Comaniciu, M. Pellkofer, and T. Koehler, "Reliable detection of overtaking vehicles using robust information fusion," *IEEE Trans. Intell. Transp. Syst.*, vol. 7, no. 4, pp. 401–414, Dec. 2006.
[7] N. Suganuma and Y. Hayashi, "Development of autonomous vehicle–overview of autonomous driving demonstration in ITS world congress 2013," in *Proc. 11th Int. Conf. Informat. Control, Autom. Robot.*, Sep. 2014, pp. 545–549.
[8] N. Suganuma and T. Uozumi, "Development of an autonomous vehicle—System overview of test ride vehicle in the Tokyo motor show 2011," in *Proc. SICE Annu. Conf. (SICE)*, Aug. 2012, pp. 215–218.
[9] J. E. Naranjo, C. Gonzalez, R. Garcia, and T. de Pedro, "Lane-change fuzzy control in autonomous vehicles for the overtaking maneuver," *IEEE Trans. Intell. Transp. Syst.*, vol. 9, no. 3, pp. 438–450, Sep. 2008.
[10] J. Perez, V. Milanes, E. Onieva, J. Godoy, and J. Alonso, "Longitudinal fuzzy control for autonomous overtaking," in *Proc. IEEE Int. Conf. Mechatronics*, Apr. 2011, pp. 188–193.
[11] N. C. Basjaruddin, K. Kuspriyanto, D. Saefudin, E. Rakhman, and A. M. Ramadlan, "Overtaking assistant system based on fuzzy logic," *Telkomnika*, vol. 13, no. 1, p. 76, 2015.
[12] D. C. K. Ngai and N. H. C. Yung, "A multiple-goal reinforcement learning method for complex vehicle overtaking maneuvers," *IEEE Trans. Intell. Transp. Syst.*, vol. 12, no. 2, pp. 509–522, Jun. 2011.
[13] X. Li, X. Xu, and L. Zuo, "Reinforcement learning based overtaking decision-making for highway autonomous driving," in *Proc. 6th Int. Conf. Intell. Control Inf. Process. (ICICIP)*, Nov. 2015, pp. 336–342.
[14] M. McNaughton, C. Urmson, J. M. Dolan, and J.-W. Lee, "Motion planning for autonomous driving with a conformal spatiotemporal lattice," in *Proc. IEEE Int. Conf. Robot. Autom.*, May 2011, pp. 4889–4895.
[15] D. Ferguson and T. M. M. Howard Likhachev, "Motion planning in urban environments," *J. Field Robot.*, vol. 25, nos. 11–12, pp. 939–960, 2008.
[16] J. Feng and J. Y. Ruan Li, "Study on intelligent vehicle lane change path planning and control simulation," in *Proc. IEEE Int. Conf. Inf. Acquisition*, Aug. 2006, pp. 683–688.
[17] S. Ulbrich and M. Maurer, "Probabilistic online POMDP decision making for lane changes in fully automated driving," in *Proc. 16th Int. IEEE Conf. Intell. Transp. Syst. (ITSC)*, Oct. 2013, pp. 2063–2067.
[18] S. Brechtel and T. R. Gindele Dillmann, "Probabilistic MDP-behavior planning for cars," in *Proc. 14th Int. IEEE Conf. Intell. Transp. Syst. (ITSC)*, Oct. 2011, pp. 1537–1542.
[19] T. Hulnhagen, I. Dengler, A. Tamke, T. Dang, and G. Breuel, "Maneuver recognition using probabilistic finite-state machines and fuzzy logic," in *Proc. IEEE Intell. Vehicles Symp.*, Jun. 2010, pp. 65–70.
[20] C. Otto and F. P. Leon, "Long-term trajectory classification and prediction of commercial vehicles for the application in advanced driver assistance systems," in *Proc. Amer. Control Conf. (ACC)*, Jun. 2012, pp. 2904–2909.
[21] M. Althoff, O. Stursberg, and M. Buss, "Model-based probabilistic collision detection in autonomous driving," *IEEE Trans. Intell. Transp. Syst.*, vol. 10, no. 2, pp. 299–310, Jun. 2009.

[22] B. Kim and K. Yi, "Probabilistic and holistic prediction of vehicle states using sensor fusion for application to integrated vehicle safety systems," *IEEE Trans. Intell. Transp. Syst.*, vol. 15, no. 5, pp. 2178–2190, Oct. 2014.

[23] L. Sun, W. Zhan, and M. Tomizuka, "Probabilistic prediction of interactive driving behavior via hierarchical inverse reinforcement learning," in *Proc. 21st Int. Conf. Intell. Transp. Syst. (ITSC)*, Nov. 2018, pp. 2111–2117.

[24] Y. Hu, W. Zhan, L. Sun, and M. Tomizuka, "Multi-modal probabilistic prediction of interactive behavior via an interpretable model," in *Proc. IEEE Intell. Vehicles Symp. (IV)*, Jun. 2019, pp. 557–563.

[25] Y. Jeong, S. Kim, and K. Yi, "Surround vehicle motion prediction using LSTM-RNN for motion planning of autonomous vehicles at multi-lane turn intersections," *IEEE Open J. Intell. Transp. Syst.*, vol. 1, pp. 2–14, 2020.

[26] S. J. Anderson, S. C. Peters, T. E. Pilutti, and K. Iagnemma, "An optimal-control-based framework for trajectory planning, threat assessment, and semi-autonomous control of passenger vehicles in hazard avoidance scenarios," *Int. J. Vehicle Auto. Syst.*, vol. 8, nos. 2–4, p. 190, 2010. 2010

[27] D. Q. Mayne, J. B. Rawlings, C. V. Rao, and P. O. M. Scokaert, "Constrained model predictive control: Stability and optimality," *Automatica*, vol. 36, no. 6, pp. 789–814, Jun. 2000.

[28] D. Q. Mayne, M. M. Seron, and S. V. Raković, "Robust model predictive control of constrained linear systems with bounded disturbances," *Automatica*, vol. 41, no. 2, pp. 219–224, Feb. 2005.

[29] G. Schildbach and F. Borrelli, "Scenario model predictive control for lane change assistance on highways," in *Proc. IEEE Intell. Vehicles Symp. (IV)*, Jun. 2015, pp. 611–616.

[30] A. Gray, Y. Gao, T. Lin, J. K. Hedrick, and F. Borrelli, "Stochastic predictive control for semi-autonomous vehicles with an uncertain driver model," in *Proc. 16th Int. IEEE Conf. Intell. Transp. Syst. (ITSC)*, Oct. 2013, pp. 2329–2334.

[31] J. Suh, H. Chae, and K. Yi, "Stochastic model-predictive control for lane change decision of automated driving vehicles," *IEEE Trans. Veh. Technol.*, vol. 67, no. 6, pp. 4771–4782, Jun. 2018.

[32] J. Li, W. Zhan, and M. Tomizuka, "Generic vehicle tracking framework capable of handling occlusions based on modified mixture particle filter," in *Proc. IEEE Intell. Vehicles Symp. (IV)*, Jun. 2018, pp. 936–942.

[33] O. Afolabi, K. Driggs-Campbell, R. Dong, M. J. Kochenderfer, and S. S. Sastry, "People as sensors: Imputing maps from human actions," in *Proc. IEEE/RSJ Int. Conf. Intell. Robots Syst. (IROS)*, Oct. 2018, pp. 2342–2348.

[34] L. Sun, W. Zhan, C.-Y. Chan, and M. Tomizuka, "Behavior planning of autonomous cars with social perception," in *Proc. IEEE Intell. Vehicles Symp. (IV)*, Jun. 2019, pp. 207–213.

[35] A. Rucco and A. P. J. Aguiar Hauser, "Trajectory optimization for constrained UAVs: A virtual target vehicle approach," in *Proc. Int. Conf. Unmanned Aircr. Syst. (ICUAS)*, Jun. 2015, pp. 236–245.

[36] M. Bibuli, M. Caccia, and L. Lapierre, "Virtual target based coordinated path-following for multi-vehicle systems," *IFAC Proc. Volumes*, vol. 43, no. 20, pp. 336–341, Sep. 2010.

[37] *Road Traffic Law*, Republic of Korea, Seoul, South Korea, 2019.

[38] T. Kondoh, T. Yamamura, S. Kitazaki, N. Kuge, and E. R. Boer, "Identification of visual cues and quantification of Drivers' perception of proximity risk to the lead vehicle in car-following situations," *J. Mech. Syst. Transp. Logistics*, vol. 1, no. 2, pp. 170–180, 2008.

[39] S. Moon and K. Yi, "Human driving data-based design of a vehicle adaptive cruise control algorithm," *Vehicle Syst. Dyn.*, vol. 46, no. 8, pp. 661–690, Aug. 2008.

[40] J. R. Sayer, M. L. Mefford, P. S. Fancher, R. E. Ervin, and S. E. Bogard, "An experimental design for studying how driver characteristics influence headway control," in *Proc. Conf. Intell. Transp. Syst.*, Nov. 1997, pp. 870–875.

[41] Q. H. Do, H. Tehrani, S. Mita, M. Egawa, K. Muto, and K. Yoneda, "Human drivers based active-passive model for automated lane change," *IEEE Intell. Transp. Syst. Mag.*, vol. 9, no. 1, pp. 42–56, 2017.

[42] R. Rajamani, *Vehicle Dynamics and Control*. New York, NY, USA: Springer, 2011.

[43] P. Falcone, F. Borrelli, J. Asgari, H. E. Tseng, and D. Hrovat, "Predictive active steering control for autonomous vehicle systems," *IEEE Trans. Control Syst. Technol.*, vol. 15, no. 3, pp. 566–580, May 2007.

[44] N. Minoiu Enache, M. Netto, S. Mammar, and B. Lusetti, "Driver steering assistance for lane departure avoidance," *Control Eng. Pract.*, vol. 17, no. 6, pp. 642–651, Jun. 2009.

[45] Y. Jeong, "Trajectory prediction of surrounding vehicles and motion planning for automated driving in urban intersections," Ph.D. dissertation, Dept. Mech. Eng., Seoul Nat. Univ., Seoul, South Korea, 2020.

[46] K. Li and P. Ioannou, "Modeling of traffic flow of automated vehicles," *IEEE Trans. Intell. Transp. Syst.*, vol. 5, no. 2, pp. 99–113, Jun. 2004.

[47] A. Domahidi and J. Jerez, *Forces Professional*. Zürich, Switzerland: embotech GmbH, 2014.

HEUNGSEOK CHAE received the B.S. degree in mechanical engineering from Seoul National University, South Korea, in 2011, where he is currently pursuing the Ph.D. degree in mechanical and aerospace engineering. His research interests are automated driving vehicle control, the motion planning of automated driving vehicles, autonomous lane change, and model predictive control.

KYONGSU YI received the B.S. and M.S. degrees in mechanical engineering from Seoul National University, South Korea, in 1985 and 1987, respectively, and the Ph.D. degree in mechanical engineering from the University of California at Berkeley, Berkeley, in 1992.

He is currently a Professor with the School of Mechanical and Aerospace Engineering, Seoul National University. His research interests are control systems, driver assistant systems, and active safety systems of ground vehicles. He currently serves as a member of the editorial boards of the KSME, IJAT, and ICROS journals.

• • •